A Full Multigrid Method for Linear Complementarity Problems arising from Elastic Normal Contact Problems

J. Zhao[1], E.A.H.Vollebregt[1,2], and C.W. Oosterlee[1,3]

[1]DIAM, Delft University of Technology, The Netherlands
[2]VORtech, Delft, The Netherlands
[3]CWI, Centrum Wiskunde and Informatica, Amsterdam, The Netherlands

Abstract

This paper presents a full multigrid (FMG) method, which combines a multigrid method, an active set algorithm and a nested iteration technique, to solve a linear complementarity problem (LCP) modeling elastic normal contact problems. The governing system in this LCP is derived from an integral equation and its coefficient matrix is dense, symmetric and block Toeplitz. An efficient and accurate initial guess of pressures and contact area is provided by the FMG method. One multigrid cycle is applied to solve this system approximately in each active set iteration. The results of our numerical experiments indicate that, on the one hand, one multigrid cycle is sufficient to obtain a satisfactory active set, and, on the other hand, our method can reduce the number of matrix-vector products and hence reduce the computational time to a great extent, compared to the original active set algorithm "NORM" developed by Kalker and implemented in his CONTACT software [13].

Keywords: full multigrid, linear complementarity problems, normal contact problem, active set algorithm, wheel-rail contact.

1 Introduction

In the simulation of the dynamic behavior of railway, the interaction between the vehicle wheels and rails attracts a lot of interest. It involves the solution of so-called *contact problems* [15], concerning the normal and tangential tractions on the inter-surface. Venner and Lubrecht [12], Willner [16] and Z.Li et al. [7], amongst many others are working on different aspects of these problems. The formulation adopted in the CONTACT software, based on the variational approach by Kalker [5], [6], [14], is regarded as an accurate model for contact problems. However, the CONTACT solution methods need improvement when a fine discretization is applied. The work in this paper focuses on the speedup, i.e. reducing the computational time for normal contact problems in which a linear complementarity problem (LCP) is solved.

The structure of this paper is as follows: in Section 2, the normal contact problem is introduced and the LCP is derived. The original active set algorithm "NORM", developed by Kalker, follows in Section 3. Section 4 illustrates our FMG method, including the multigrid-based algorithm, each component of the multigrid method and the FMG approach in general. Numerical experiments with results are shown in Section 5, and the conclusions and future work will be summarized in the end.

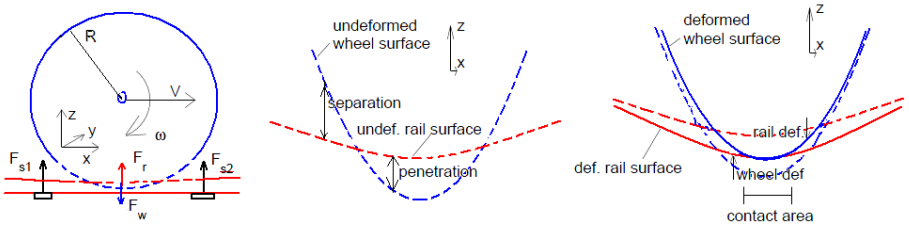

Figure 1: Geometry of contact problems

2 Problem formulation

2.1 Normal contact problem

When the surfaces of two bodies roll over each other, a contact area occurs between them, carrying normal and tangential tractions. An elastic field of displacements, strains, and stresses in the bodies also appears with these tractions, all of which result in deformations [6]. The tractions are the main issue we are solving for. In the *normal contact problem*, the forces of the contacting bodies are perpendicular to the surface [10] and we only consider the normal tractions (pressures) here.

Figure 1 shows the general geometry of this contacting phenomenon. The left graph is the overall geometry, displaying a wheel rolling on the rail with a forward velocity v and angle velocity ω. The rail is deformed caused by the forces from the wheel, F_w, and from the sleepers, F_{s1}, F_{s2}. At the same time, the wheel has deformation due to the force from the rail, F_r. Now we stretch this graph vertically in order to have an insight look at this phenomenon. The graphs of the wheel and rail in the middle and on the right give the undeformed state and deformed state, respectively. A contact area occurs where the surfaces of the wheel and rail coincide, while the distance between their surfaces is positive outside the contact area with no tractions there. Let C denote the contact area and E the exterior area. Then, the *contact conditions* for normal contact problems are:

$$e(x,y) = 0,\ p(x,y) \geq 0, \qquad \text{for a position} \quad (x,y) \in C, \tag{2.1}$$

$$e(x,y) > 0,\ p(x,y) = 0, \qquad \text{for a position} \quad (x,y) \in E, \tag{2.2}$$

where $p(x,y)$ is the normal traction, i.e. pressure, and $e(x,y)$ is the deformed distance between the wheel and rail, at position (x,y). Let $h(x,y)$ denote the undeformed distance at (x,y), then the deformed distance, $e(x,y)$, can be defined by:

$$e(x,y) = h(x,y) + u(x,y), \tag{2.3}$$

where $u(x,y)$ is the deformation. This equation will be defined for all positions in the contact area C and noticing that the deformed distance $e(x,y) = 0$ for position $(x,y) \in C$, equation (2.3) results in:

$$u(x,y) = -h(x,y), \quad \text{for a position} \quad (x,y) \in C. \tag{2.4}$$

2.2 The half-space approach

The method to calculate the deformation u is based on three simplifying assumptions in Kalker's variational approach [6]. First of all, the contact area is considered very small compared to the two contacting bodies, and hence this area is considered to be flat. The second is that the contacting

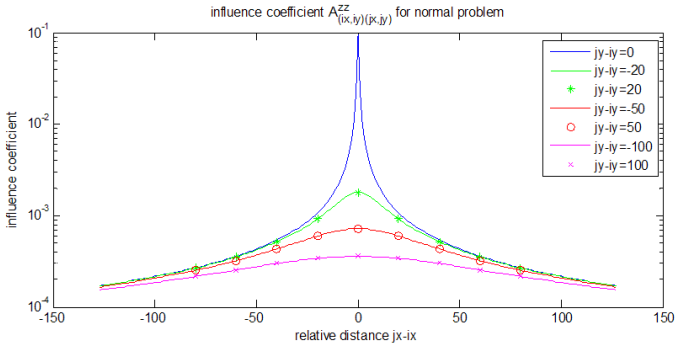

Figure 2: Influence coefficient $A^{zz}_{(ix,iy)(jx,jy)}$

bodies are assumed to be made of homogeneous linear elastic material. The last assumption is to ignore inertial effects in the motion.

These assumptions allow the use of the *half-space approach*, which approximates the elastic field of two contacting bodies considering each body as a *semi-infinite elastic solid* bounded by a plane surface. Based on the classic solutions by Boussinesq and Cerruti (see Johnson [4]) and considering the normal contact problems, we give the normal traction-deformation relation, as follows:

$$u^z(x,y) = \int\int_C A^{zz}(x,y,\xi,\eta)p^z(\xi,\eta)d\xi d\eta, \tag{2.5}$$

where z denotes the normal direction, u^z and p^z are the normal deformation and pressure, respectively, and $A^{zz}(x,y,\xi,\eta)$ is the influence function for normal deformation at the surface position (x,y) due to the contribution of a unit pressure at surface position (ξ,η). This influence function is calculated by:

$$A^{zz}(x,y,\xi,\eta) = \frac{1-\nu}{\pi G}\cdot\frac{1}{\rho}, \tag{2.6}$$

where ν and G are the Poisson ratio and shear modulus, respectively, and ρ is the distance between points (x,y) and (ξ,η), i.e., $\rho = [(x-\xi)^2 + (y-\eta)^2]^{\frac{1}{2}}$.

2.3 Discretization

Solving contact problems often starts with the discretization of a potential contact area, which contains the true contact area. The potential contact area is discretized by $m_x \cdot m_y$ rectangular elements of size $\delta x \cdot \delta y$. Each element is numbered by (ix, iy) where $1 \le ix \le m_x$ and $1 \le iy \le m_y$.

A piecewise constant function per element is used to approximate the surface pressures. Then the discretization of integral (2.5) gives:

$$u^z_{(ix,iy)} = \sum_{iy}^{m_y}\sum_{ix}^{m_x} A^{zz}_{(ix,iy)(jx,jy)}p^z_{(jx,jy)}, \tag{2.7}$$

where the subscript (ix, iy) denotes the element. Influence coefficient $A^{zz}_{(ix,iy)(jx,jy)}$ is calculated by integrating (2.5) for a unit traction in a single element (jx, jy) w.r.t. an observation point at the center of element (ix, iy). It has the property that $A^{zz}_{(ix,iy)(jx,jy)} = A^{zz}_{(kx,ky)(lx,ly)}$ when $jx - ix = lx - kx, jy - iy = ly - ky$, i.e. the coefficients are identical for pairs of elements which

have the same relative distance. Figure 2 shows the influence coefficients scaled by G for the test problem in Section 5.1.

If we use an $m_x \times m_y$ grid and let $N = m_x \cdot m_y$, equation (2.7) defined by the potential contact area gives the equation:

$$\vec{u} = A\vec{p}, \quad \vec{p}, \vec{u} \in \mathbb{R}^N, A \in \mathbb{R}^{N \times N}, \tag{2.8}$$

where the influence coefficient matrix, A, is a dense, symmetric and block Toeplitz matrix. Combining equations (2.3) and (2.8) leads to the main equation in the normal contact problem:

$$\vec{e} = \vec{h} + A\vec{p}. \tag{2.9}$$

From the above discussion, we consider equation (2.9) and the contact conditions (2.1) and (2.2). This results in a linear complementarity problem LCP(h, A), which aims to find the pressures, $\vec{p}$, contact area, C, and exterior area, E, satisfying

$$\begin{cases} \vec{e} = \vec{h} + A\vec{p} & (2.10) \\ e_I = 0, p_I \geq 0, \quad \text{for element} \quad I \in C, & (2.11) \\ e_I > 0, p_I = 0, \quad \text{for element} \quad I \in E, & (2.12) \end{cases}$$

where I is the element index calculated by $I = (iy - 1) \cdot m_x + ix$ and $1 \leq I \leq N$. Note that the constraints on the deformed distance $\vec{e}$ are the primary constraints: $e_I = 0$ defines the active constrains and $e_I > 0$ are inactive constraints. This LCP represents a mathematical model for normal contact problems. We will discuss the original method and the FMG method for solving it in the following sections.

3 Original method: Active set algorithm

The active set algorithm is well-known for optimization problems, such as the LCP problem above. The main idea is to partition the inequality constraints into two groups, i.e. an active and inactive set. Those parts that satisfy the constraints are put in the active set and the others are in the inactive set. Only the active set is considered when solving the equality problem. One active set iteration has two components, i.e. first to determine a current active set as the working set, and then solve the equality problem in this active set. These two steps are repeated until all the constraints or conditions are satisfied [9].

For the contact problem, the contact area is regarded as the active set and the exterior area is the inactive set. The original algorithm has the following structure:

1. Find a starting active set, i.e. the initial contact area C^0. After the discretization of the potential contact area, we obtain an initial contact area C^0 consisting of every element I which satisfies the condition $h_I \leq 0$.

2. The Conjugate Gradient method is applied to solve the linear system (2.10) defined by the current contact area C^k. Note that the $N \times N$ system is "reduced" by inserting $p_I = 0$ for the elements I in the exterior area E^k.

3. Solution $\vec{p}$ and deformed distance $\vec{e}$ are used, according to the contact conditions (2.11) and (2.12), to determine a new contact area C^{k+1}.

4. If the new contact area C^{k+1} is different from C^k, repeat 2 and 3. Otherwise, we have found the correct contact area C^{k+1} and the pressures on it.

From the above algorithm, we see that, in each active set iteration, we have to solve one linear system (2.10). On the one hand, this system will be large and has a dense system matrix. Note that this matrix is not Toeplitz anymore. On the other hand, several active set iterations are needed before the correct contact area is obtained, which means that we have to solve many different systems. Hence, these two facts cause slow computation.

4 A Full Multigrid method

4.1 Multigrid-based algorithm

Notice that, when we examine the contact conditions, we do not need the exact values of deformed distance $\vec{e}$ or pressures $\vec{p}$, since the conditions only focus on whether these values are positive, negative or zero. Therefore, we arrive at an approach to solve system (2.10) approximately, by one multigrid cycle, instead of the Conjugate Gradient method. This idea combined with the active set algorithm results in our *multigrid-based algorithm*, which is described as follows:

1. We start with a discretization for the potential contact area. Check undeformed distance $\vec{h}$: put the element I satisfying $h_I \leq 0$ in the initial contact area C^0.
2. Set the pressures in the exterior area E^k to zero, and define the system (2.10) by restricting to the current contact area C^k.
3. Apply one multigrid cycle to this system, and obtain the pressures $\vec{p}$.
4. Check the contact conditions:
   (4.1) Consider each element I in the contact area C^k. If the pressure $p_I < 0$ then put element I to the exterior area and set $p_I = 0$. This leads to the contact area $\overline{C}^{k+1}$ and exterior area $\overline{E}^{k+1}$.
   (4.2) Consider each element I in the exterior area $\overline{E}^{k+1}$. Put the element I into the contact area C^{k+1} with its deformed distance $e_I = h_I + u_I \leq 0$.
   Now a new contact area, C^{k+1}, and exterior area, E^{k+1}, have been obtained.
5. If this new contact area C^{k+1} is different from the previous area C^k, then go to step 2. If not, go to step 6.
6. If the solution is not of the required accuracy, then go to step 2. Otherwise, stop and we have found a converged contact area and the pressures on it.

Here, superscript k denotes the iteration number of the active set algorithm. In this algorithm, the multigrid method plays a crucial role. We will give more details about its components.

4.2 Multigrid components

Multigrid is one of the most efficient numerical solvers for systems of equations arising from elliptic PDEs, but we will use the multigrid algorithm to deal with the system (2.10), which has a dense coefficient matrix, in an active set iteration. Our work is closely related to that of Brandt, Lubrecht

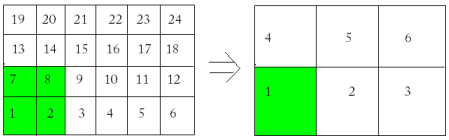

Figure 3: Standard coarsening means combining 2×2 cells into 1 coarse grid cell. For example, the green element 1 on the coarse grid is obtained by combining four green elements 1,2,7,8 on the fine grid.

and Venner, and their co-workers, as presented, for example, in [8, 2, 1, 12]. Since, according to the contact conditions, the pressures in the exterior area are always zero, we keep these pressure unchanged. A two-grid algorithm is given below. It is easy to extend it to a multigrid algorithm.

- Pre- and post- smoothing: We use the damped Gauss-Seidel method as the smoother. Notice that we only deal with the pressures on the elements within the contact area C_h^k, because the pressures in the exterior area E_h^k are fixed to zero.
- Calculate defects: The defects in the contact area, C_h^k, are computed, and the defects in the exterior area E_h^k are set to zero. This gives us the fine grid defects, d_h.
- Restrict the defects, d_h, and contact area, C_h^k, to the coarse grid, resulting in coarse grid defects, d_H, and a coarse contact area, C_H^k, respectively.
- On the coarse grid: Apply an exact solver, i.e. a Gauss elimination method, for the defect equation, $A_H \overline{v}_H = d_H$, defined by the coarse contact area, C_H^k. The coarse grid correction, v_H, satisfies $v_H = \overline{v}_H$ in C_H^k, and $v_H = 0$ in E_H^k.
- Interpolate the coarse grid correction v_H to the fine grid, yielding the fine grid correction v_h, and set $v_h = 0$ in the exterior area E_h^k.
- Correction: Add correction, v_h, to the smoothed pressures, p_h, for all the elements in the potential contact area.

Here, the subscripts h and H denote the fine and coarse grid, respectively. From this algorithm, we can see that both systems (2.10) and $A_H \overline{v}_H = d_H$ are defined on the contact areas C_h^k and C_H^k, respectively. All the quantities in the exterior areas, E_h^k and E_H^k, are set equal to zero in this algorithm, to satisfy the contact condition that $p_I = 0$ for all the elements I in the exterior area.

The idea for coarsening is the simple and most frequently used choice, *standard coarsening*, i.e. doubling the element size in each direction. An example is depicted in Figure 3, where all the elements are numbered in lexicographic ordering. The strategy of restriction and interpolation is described based on the green elements in Figure 3.

- Restriction of defects: the average of defects of four elements, for example 1,2,7 and 8, becomes the defect for an element, 1, on the coarse grid, i.e. $d_H^1 = \frac{1}{4}(d_h^1 + d_h^2 + d_h^7 + d_h^8)$, where d is defect, h and H denote the grid size ($H = 2h$), and the superscripts denote the element numbers.
- Restriction of the contact area: among the elements 1,2,7,8, if there are 2 or more elements in the contact area C_h, then the coarse grid element 1, which is obtained by combining these four elements, is in the coarse contact area C_H.

- Interpolation of the correction: the correction of coarse element 1, i.e. v_H^1, is the correction of each of the four fine grid elements, 1,2,7,8, i.e. $v_H^1 = v_h^1 = v_h^2 = v_h^7 = v_h^8$.

4.3 The FMG scheme

In addition to the multigrid-based algorithm described above, we also incorporated the idea of nested iteration, which results in a *full multigrid* method. On the coarsest grid, we solve the LCP by the original active set algorithm with the CG method, to obtain the coarse pressures $\vec{p}$ and deformation $\vec{u}$. Then, we interpolate them to a finer grid, where the deformed distance, $\vec{e}$, is calculated, yielding an initial contact area on this grid level. We solve the LCP on the current grid level by the active set algorithm using one multigrid iteration, and repeat this procedure until we reach the finest grid, where the multigrid algorithm is applied. The details of this FMG scheme will be given in the full version of this paper. We will provide a numerical result here.

5 Numerical experiment and results

5.1 Test problem

This test is a 'Hertzian' case [3]. The undeformed distance function is $h(x, y) = a_1x^2 + b_1y^2 - pen$, where $a_1 = 0.0016681/mm$ is the combined curvature in x-direction, $b_1 = 0.0030671/mm$ is the combined curvature in y-direction and $pen = 0.1091\ mm$ is the maximum inter-penetration of the undeformed profiles. The potential contact area is $(x, y) \in [-10, 10] \times [-6, 6]\ mm^2$, and steel material with shear modulus $G = 82000N/mm^2$ and the Poisson ratio $\nu = 0.28$ is used to calculate the coefficient matrix A in system (2.10). We solve for the contact area, C, and the corresponding pressures.

Hertz gave an analytic solution to the normal contact problems in [3]. The contact area is elliptic. For steel material in this test problem, the semi-axes of the contact ellipse are $a_2 = 6.0\ mm, b_2 = 4.0\ mm$, where a_2 and b_2 are half widths of the contact ellipse in the x- and y-directions, respectively. The normal pressure is zero outside the contact ellipse. In the contact area, it has "semi-ellipsoidal" form: $p_n(x, y) = p_{max} \cdot \sqrt{1 - (\frac{x}{a_2})^2 - (\frac{y}{b_2})^2}$, where the maximum pressure, $p_{max} = 3F_n/(2 \cdot \pi \cdot a_2 \cdot b_2) = 1631N/mm^2$, with total load $F_n = 82000N$.

5.2 Results by the multigrid solver

We first analyze the multigrid solvers numerically to determine the efficiency of the multigrid components. The system we will solve here is called the C^1 *system*, which is (2.10) defined by the initial contact area. In this test, the C^1 system will be solved to a high accuracy, not approximately.

We implement the multigrid V(1,1)-cycle with the following smoothers: standard Gauss-Seidel, red-black Gauss Seidel, Jacobi, damped Jacobi, damped Gauss-Seidel, with $\omega > 1$ (SOR) and $\omega < 1$ (SUR). The multigrid methods use 4×4 as the coarsest grid. The iterations stop when $\frac{\|r\|_2}{\|h\|_2} \leq 10^{-6}$, which are the 2-norms of the residual and the right-hand side of the system (2.10), respectively.

We found, first of all, that the multigrid methods with Jacobi and damped Jacobi smoothers did not converge, when a fine discretization was used. Moreover, red-black Gauss-Seidel showed worse convergence than the standard Gauss-Seidel smoother for system (2.10). We do not show these results here.

Discretization	$\omega = 1.1$	$\omega = 0.8$	$\omega = 1$	CG
64×64	10 (0.2428)	9(0.1927)	9 (0.2077)	29
128×128	11(0.2783)	9(0.1974)	10(0.2402)	61

Table 1: The number of iterations by multigrid with different smoothers and by CG to solve C^1 system. The convergence factors of multigrid are given in brackets.

Table 1 presents the number of iterations obtained by multigrid with SOR ($\omega = 1.1$), SUR ($\omega = 0.8$), and standard Gauss-Seidel ($\omega = 1$) as the smoothers and the Conjugate Gradient method (CG), for different discretization resolutions. It can be seen that the Gauss-Seidel smoother with $\omega = 0.8$ requires only 9 iterations, which is the least compared to the other methods on a 128×128 grid.

The convergence factor in brackets in the table is defined as in [11]: $\widehat{q}^{(m)} = \sqrt[m]{\frac{\|d_h^m\|}{\|d_h^0\|}}$, in some appropriate norm, i.e. the 2-norm in our case. The quantity $\widehat{q}^{(m)}$ is an average residual reduction factor over m iterations, so it may be a good estimate of the multigrid convergence, if m is sufficiently large. The smaller the convergence factor, the better the convergence performance. In our test, m is chosen to be the total number of iterations for which the system is solved. From the table, we find again that the Gauss-Seidel method with $\omega = 0.8$ is the best choice for the smoother, since its convergence factor is the smallest. We will analyze the multigrid performance for the dense matrix system in more detail in the full version of this paper.

5.3 Results by multigrid-based algorithm

We arrive at the analysis of the multigrid-based algorithm to solve the LCP (2.10)-(2.12). We choose the Gauss-Seidel method with $\omega = 0.8$ as the smoother, and compare multigrid V(1,1)-, V(0,1)- and V(1,0)-cycles. The stopping criterion $\frac{\|r\|_2}{\|h\|_2} \leq 10^{-6}$ is also used here. Table 2 presents the total number of multigrid iterations with the number of matrix-vector products in brackets, by different multigrid cycles on different grids. The coarsest grid is 4×4 for each case. The number of CG iterations of the original algorithm is given as a comparison. For example, in the case of the 128^2-discretization, the original algorithm requires 8 active set iterations (not shown in the table) with a total of 198 CG iterations. It can be seen from the table that the multigrid-based algorithms require considerably fewer iterations than the original method, and this fact is more pronounced on finer grids.

Since the total number of matrix-vector products plays a prominent role regarding the computational time, we make a comparison between the multigrid-based algorithm and the original active set algorithm. We focus on the number of matrix-vector products on the finest grid, since this takes most computational time. In our algorithm, one V(1,1) cycle calculates 3 such products: one for both pre- and post- smoothers, and one to compute the defect. The Conjugate Gradient method calculates 1 product in each CG iteration. The results are also shown in brackets in Table 2. Let the factor a denote the ratio of matrix-vector product numbers by the original active set algorithm compared to the multigrid-based algorithm. Then, when using the V(1,1)-cycle, for the 32^2-, 64^2, 128^2- and 256^2-discretizations, factor a is approximately 2.9, 4.4, 6.6 and 7.8, respectively. As expected, these numbers increase as the discretization gets finer. Hence, the multigrid-based algorithm shows that the computational time can be reduced to a great extent. Moreover, one multigrid iteration is sufficient to give a satisfactory contact area for our present test case.

Discretization	V(1,1)	V(1,0)	V(0,1)	CG
32×32	9(27)	16(32)	16(32)	77(77)
64×64	10(30)	17(34)	16(32)	131(131)
128×128	10(30)	17(34)	16(32)	198(198)
256×256	12(36)	20(40)	28(56)	280(280)

Table 2: The total number of multigrid iterations by the multigrid-based algorithm and the CG iterations in the original active set algorithm, with the number of matrix-vector products in brackets

Discretization	V(1,1)	V(1,0)	V(0,1)
32×32	7(21)	13(26)	13(26)
64×64	6(18)	11(22)	12(24)
128×128	5(15)	9(18)	9(18)
256×256	6(18)	10(20)	8(16)

Table 3: The total number of multigrid iterations by the FMG method and the CG iterations in the original active set algorithm, with the number of matrix-vector products in brackets

5.4 Results by the FMG method

Now we combine the multigrid method with the FMG technique and present the convergence results on the finest grid in Table 3. We find that the number of FMG iterations and matrix-vector products are fewer when the FMG technique is applied, compared with the results in Table 2. And now the factor a is approximately 3.7, 7.3, 13.2 and 15.6 when using the V(1,1)-cycle for the 32^2-, 64^2, 128^2- and 256^2-discretizations, respectively.

A comparison is made of the difference between the initial contact areas and the true contact area when solving the LCP (2.10)-(2.12) on a 32^2-grid, which is shown in Figure 4, where the blue spots denote the elements in the contact area and yellow represents the exterior area. It can be seen from the figure that the initial contact area, using the FMG scheme (in (b)) resembles much better the true contact area (in (c)), than the original method which was based on the initial contact area (in (a)).

6 Conclusions and future work

In this paper, we presented a full multigrid method, which is a combination of a multigrid method, an active set algorithm and the nested iteration approach, to solve linear complementarity prob-

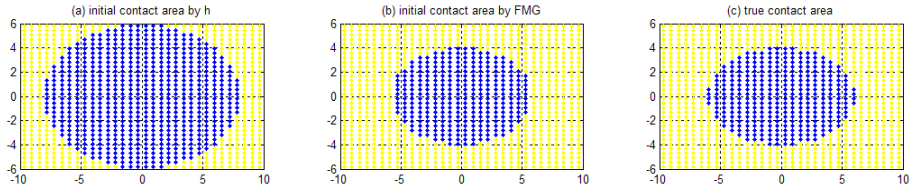

Figure 4: Contact areas on 32×32 grid: (a) the initial contact area obtained by selecting all the elements I with $h_I \leq 0$, (b) the initial contact area by the FMG scheme, (c) the true contact area

lems arising from elastic normal contact problems. Multigrid shows its efficiency for solving the corresponding integral equations, which exhibit a dense coefficient matrix. In our test case, one multigrid iteration appears to be sufficient to give an approximate solution to modify the contact areas efficiently and accurately. The FMG scheme helps to give not only more accurate initial pressures when solving system (2.10), but also provides a satisfactory initial contact area, resembling the true contact area better than the present initial contact area. Compared with the original active set algorithm in the CONTACT software, the FMG method can reduce the computational time to a factor of 3.7 to 15.6 depending on the problem size. All of the three multigrid cycles V(1,1), V(1,0) and V(0,1) perform very well, but V(1,1) seems to be the most robust method.

The future work will focus on four subjects. First of all, (local Fourier) analysis of multigrid convergence should be part of our work, to understand the multigrid performance from a theoretical perspective. Secondly, the fact that the coefficient matrix of the system is a block Toeplitz matrix may allow us to employ the Fast Fourier Transform as a multigrid smoother in the algorithm. Thirdly, we will apply our algorithm to more complicated situations. For example, if the contacting surface is rough due to wear of the wheel and rail, then the true contact area consists of several small irregular domains, instead of a simple ellipse. The above issues are still considered for the normal contact problems. In the near future, however, we will also study the tangential contact problems, for which more detailed solutions are demanded for railway applications.

References

[1] A. Brandt, C.W. Cryer, Multigrid algorithms for the solution of linear complementarity problems arising from free boundary problems.

[2] A. Brandt, A.A. Lubrecht, Multilevel matrix multiplication and fast solution of integral equations, *J. Comput. Phys.,* 90: 348370, 1990. *SIAM J. Sci. Comput.* 4: 655-684, 1983.

[3] H. Hertz, 'Über die Berührung fester elastischer Körper,' *Journal fur reine und angewandte Mathematik*, 92, 1882,pp.156-171.

[4] K.L.Johnson, 'Contact Mechanics,' *Cambridge University Press, Cambridge (UK)*, 1985.

[5] J. Kalker, 'The computation of Three-Dimensional Rolling Contact with Dry Friction, '*Int. Journ. for Numerical Methods in Engineering*,14:1293-1307,1979.

[6] J.J.Kalker, 'Three-Dimensional Elastic Bodies in Rolling Contact,' *Solid Mechanics and its Applications,Kluwer Academic Publishers*, 1990.

[7] Z. Li, X. Zhao, C. Esveld,R. Dollevoet and M. Molodova, 'An investigation into the causes of squatsCorrelation analysis and numerical modeling', *Wear, Elsevier*, 265:1349-1355,2008.

[8] A.A. Lubrecht, C.H. Venner, W.E. ten Napel, and R. Bosma, Film thickness calculations in a Elastohydrodynamically Lubricated Circular Contacts, Using a Multigrid Method, *ASME J. of Tribology*, 110: 503-507, 1988.

[9] K.G. Murty, ' Linear complementarity, linear and nonlinear programming', *Sigma Series in Applied Mathematics. 3. Berlin: Heldermann Verlag*,1998.

[10] Valentin L.Popov, 'Contact Mechanics and Friction, Physical Principles and Applications,' *Springer*,2010

[11] U. Trottenberg. C.W. Oosterlee, A. Schüller. Multigrid *Academic Press*,2001.

[12] C.H.Venner and A.A.Lubrecht, Multilevel methods in lubrication, *Elsevier* 2000.

[13] E.A.H.Vollebregt, 'Survey of programs on contact mechanics developed by J.J.Kalker', *Vehicle System Dynamics,*, 46:1-2,85-92,2008.

[14] E.A.H.Vollebregt, 'User's Guide for CONTACT, J.J. Kalker's variational contact model,' Technical Report TR09-03, VORtech, P.O. Box 260, 2600 AG Delft, 2009, ww.kalkersoftware.org.

[15] E.A.H.Vollebregt, S.D.Iwnicki, G.Xie and P.Shackleton 'Assessing the accuracy of different simplified frictional rolling contact algorithms,' *vehicle System Dynamics*, 50:1,1-17,2012.

[16] K. Willner, 'Elasto-Plastic Normal Contact of Three-Dimensional Fractal Surfaces Using Halfspace Theory', *ASME J. Tribol.* 126: 28-33, 2004.